^{19}F NMR study of $LiTbF_4$ single crystals

2011 J. Phys.: Conf. Ser. 324 012034

(http://iopscience.iop.org/1742-6596/324/1/012034)

^{19}F NMR study of $LiTbF_4$ single crystals

I V Romanova, A V Egorov, S L Korableva, B Z Malkin and M S Tagirov

Kazan Federal University, Kremlevskaya 18, 420008 Kazan, Russia

E-mail: Irina.Choustova@ksu.ru

Abstract. The angular dependences of ^{19}F NMR spectra have been measured in the external magnetic field of 0.5 T oriented in the basis plane of $LiTbF_4$ at the room temperature. We have obtained the constants of transferred hyperfine interaction and the corrected set of crystal field parameters for the Tb^{3+} ions in $LiTbF_4$. The results of simulations of the magnetization in high pulsed magnetic fields with taking into account magnetoelastic interactions agree satisfactorily with experimental data presented in the literature.

1. Introduction

Double lithium rare-earth fluorides crystallizing in the tetragonal scheelite ($CaWO_4$) structure (C_{4h}^6) attract much attention as model objects in physics of magnetism [1]. The unit cell of $LiRF_4$ contains two magnetically equivalent lanthanide R^{3+} ions at sites with the S_4 point symmetry. $LiTbF_4$ is a dipolar Ising-like ferromagnet (T_c=2.89 K) [2]. Earlier ^{19}F NMR in this material at 295 K was studied by Hansen et al. [3], and they determined parameters of the transferred hyperfine interactions between the Tb^{3+} ions and the ^{19}F and ^{7}Li nuclei. The sets of transferred hyperfine interaction constants were obtained from fitting the calculated NMR spectra to the experimental data. The local magnetic fields induced by Tb^{3+} magnetic moments at ^{19}F nuclei were calculated using bulk magnetic susceptibilities of $LiTbF_4$ measured in [4, 5].

In general case, temperature variations of local magnetic fields in a paramagnetic crystal can be calculated if parameters of the crystal field affecting paramagnetic ions are known. However, different sets of the crystal field parameters have been introduced in the literature to describe magnetic and spectral properties of $LiTbF_4$ [6, 7] and terbium doped isomorphic $LiYF_4$ crystals [8, 9]. Earlier we studied temperature and magnetic field dependences of the magnetization of $LiRF_4$ single crystals (R=Dy, Ho, Tb) [10, 11] taking into account magnetoelastic interactions and found corrected sets of the crystal field parameters for Tb^{3+}, Dy^{3+} and Ho^{3+} ions. It should be noted that in theoretical studies of $LiTbF_4$ spectral properties carried out earlier, as well as in our previous work [11], crystal field energies of the Tb^{3+} ion were calculated by making use of the ion Hamiltonian acting in the truncated space of electronic states belonging to the ground $4f^8$ configuration. This resulted in remarkable differences between some crystal field parameters obtained for stoichiometric $LiTbF_4$ [6, 7, 11] and for the impurity Tb^{3+} ions in $LiYF_4$ [8, 9]. To determine unambiguously the total set of seven crystal field parameters (in crystallographic frame) for rare earth ions at the sites with the S_4 symmetry, it is necessary to analyze responses of the ions on large enough direction dependent perturbations (in particular, on external magnetic fields). In the present work we use additional information about the local magnetic fields in $LiTbF_4$ obtained from ^{19}F NMR spectra and the results of the magnetization measurements in high pulsed magnetic fields [12], as well as more precise technique of calculations of the terbium magnetic moments, in order to validate different parameters of the microscopic model

describing static and dynamic magnetic properties of $LiTbF_4$. Theoretical grounds for simulations of the local magnetic fields are considered in section 2 of the present work, and in section 3 we analyze the results of ^{19}F NMR measurements.

2. Magnetic moment of the Tb^{3+} ion in $LiTbF_4$ in external magnetic field

To calculate the angular dependence of the ^{19}F NMR spectra, we need to know local magnetic fields affecting the ^{19}F nuclei. Local fields depend on the average values of the Tb^{3+} magnetic moments. The magnetic moments of the Tb^{3+} ions are considered here with taking into account interactions of the Tb^{3+} ion with the static crystal field and lattice deformations and magnetic (dipole-dipole and exchange) interactions between the Tb^{3+} ions.

In the presence of an applied magnetic field $\boldsymbol{B}$ (below a direction of $\boldsymbol{B}$ relative to the crystallographic axes is specified by spherical coordinates θ (the angle between $\boldsymbol{B}$ and the *c*-axis) and φ (the angle between the $\boldsymbol{B}$ projection onto the *ab*-plane and the [100] axis)), we write down the Hamiltonian of a single Tb^{3+} ion in the following form (the nuclear Zeeman energy and the hyperfine interaction are neglected):

$$H = H_0 + H_{cf} - \mu_B \boldsymbol{B}_{loc}(\boldsymbol{L} + 2\boldsymbol{S}) + \sum_{\alpha\beta} V'_{\alpha\beta} e_{\alpha\beta} + \sum_{\alpha,s} V''_{\alpha}(s) w_{\alpha}(s) . \quad (1)$$

The Hamiltonian (1) operates in the total space of 3003 states of the electronic $4f^8$ configuration, the first term is the free ion Hamiltonian, the second term is the crystal field Hamiltonian:

$$H_{cf} = B_2^0 O_2^0 + B_4^0 O_4^0 + B_4^4 O_4^4 + B_4^{-4} \Omega_4^4 + B_6^0 O_6^0 + B_6^4 O_6^4 + B_6^{-4} \Omega_6^4 \quad (2)$$

determined in the crystallographic system of coordinates by the set of seven crystal field parameters B_p^k (O_p^k and Ω_p^k are the linear combinations of spherical tensor operators similar to the corresponding Stevens operators [13]). The third term in (1) is the electronic Zeeman energy (μ_B is the Bohr magneton, $\boldsymbol{L}$ and $\boldsymbol{S}$ are the electronic orbital and spin moments, respectively, and $\boldsymbol{B}_{loc}$ is the local magnetic field defined below). The last two terms define linear interactions of rare earth ions with the homogeneous macro- and microdeformations, respectively, where $\hat{\boldsymbol{e}}$ is the deformation tensor, and $\boldsymbol{w}(s)$ is the vector of the *s*-sublattice displacement. The electronic operators $V'_{\alpha\beta}$ and $V''_{\alpha}(s)$ can be represented, similar to the crystal field energy, through the linear combinations of spherical tensor operators with the parameters which have been calculated earlier in the framework of the exchange charge model [14-16]. Below we consider the electron-deformation interaction (last two terms in (1)) as a perturbation and take into account the corresponding contributions of the first order in deformation parameters $\hat{\boldsymbol{e}}$ and $\boldsymbol{w}(s)$ into the free energy of the magnetic subsystem.

The energy of a deformed crystal lattice (per unit cell with the volume v_0) is written as [16]

$$E_{lat} = \frac{v_0}{2} \hat{\boldsymbol{e}} \hat{\boldsymbol{C}}' \hat{\boldsymbol{e}} + \sum_s \boldsymbol{w}(s) \hat{\boldsymbol{b}}(s) \hat{\boldsymbol{e}} + \frac{1}{2} \sum_{ss'} \boldsymbol{w}(s) \hat{\boldsymbol{a}}(s,s') \boldsymbol{w}(s') \quad (3)$$

where $\hat{\boldsymbol{a}}$ is the dynamic matrix of the lattice at the Brillouin zone center, and the tensor of elastic constants is $\hat{\boldsymbol{C}} = \hat{\boldsymbol{C}}' - \sum_{ss'} \hat{\boldsymbol{b}}(s) \hat{\boldsymbol{a}}^{-1}(s,s') \hat{\boldsymbol{b}}(s') / v_0$. Taking into account the equilibrium conditions for the coupled paramagnetic ions and the elastic lattice, we obtain the lattice macrodeformation induced by the magnetic field

$$\hat{\boldsymbol{e}}(\boldsymbol{B}) = -\frac{n}{v_0} \hat{\boldsymbol{S}} [\langle \boldsymbol{V} \rangle_B - \langle \boldsymbol{V} \rangle_0] \quad (4)$$

and the sublattice displacements

$$\Delta \boldsymbol{w}(\boldsymbol{B}) = \boldsymbol{w}(\boldsymbol{B}) + \hat{\boldsymbol{a}}^{-1} \hat{\boldsymbol{b}} \hat{\boldsymbol{e}}(\boldsymbol{B}) = -n \hat{\boldsymbol{a}}^{-1} [\langle \boldsymbol{V}'' \rangle_B - \langle \boldsymbol{V}'' \rangle_0] . \quad (5)$$

Here $n = 2$ is the number of rare earth ions in the unit cell, $\hat{\boldsymbol{S}} = \hat{\boldsymbol{C}}^{-1}$ is the compliance tensor of the lattice, and angular brackets $<\ldots>_B$ and $<\ldots>_0$ indicate thermal averages over the eigenstates of the

Hamiltonian (1) for $\boldsymbol{B}\neq 0$ and $\boldsymbol{B}=0$, respectively. Operators $\boldsymbol{V}=\boldsymbol{V}'-\hat{\boldsymbol{b}}(s)\hat{\boldsymbol{a}}^{-1}(s,s')\boldsymbol{V}''(s')$ in (4) equal to operators $\boldsymbol{V}'$ renormalized due to linear coupling between macro- and microdeformations.

Table 1. Coupling constants (in cm^{-1}) of the electron-deformation interaction [16, 17].

	$a_{\lambda,2}^{\ 0}$	$a_{\lambda,4}^{\ 0}$	$a_{\lambda,4}^{\ 4}$	$a_{\lambda,4}^{\ -4}$	$a_{\lambda,6}^{\ 0}$	$a_{\lambda,6}^{\ 4}$	$a_{\lambda,6}^{\ -4}$	
$A_g^{\ 1}$	350	140	2300	1550	90	700	300	
$A_g^{\ 2}$	-900	500	2400	795	-50	1300	1100	
	$b_{\lambda,2}^{\ 2}$	$b_{\lambda,2}^{\ -2}$	$b_{\lambda,4}^{\ 2}$	$b_{\lambda,4}^{\ -2}$	$b_{\lambda,6}^{\ 2}$	$b_{\lambda,6}^{\ -2}$	$b_{\lambda,6}^{\ 6}$	$b_{\lambda,6}^{\ -6}$
$B_g^{\ 1}$	1644	1846	-454	1885	188	-543	-858	-738
$B_g^{\ 2}$	3814	-836	-1532	1424	-243	-658	-1444	-1245

To take into account magnetic dipole-dipole and exchange interactions between the rare earth ions, we use the mean field approximation. The local field in the spherical sample equals

$$\boldsymbol{B}_{loc}=\boldsymbol{B}+(\hat{\boldsymbol{Q}}+\hat{\boldsymbol{\lambda}}-N\hat{\boldsymbol{I}})\boldsymbol{M} \tag{6}$$

($\hat{\boldsymbol{Q}}$ is the tensor of dipole lattice sums, the tensor $\hat{\boldsymbol{\lambda}}$ determines the exchange field, the demagnetizing factor $N=4\pi/3$, $\hat{\boldsymbol{I}}$ is the unit tensor, $\boldsymbol{M}$ is the magnetization). We substitute expressions (4) and (5) for $\hat{\boldsymbol{e}}$ and $\boldsymbol{w}(s)$, respectively, in (1) and thus obtain the effective self-consistent single-ion Hamiltonian $H_{eff}(\boldsymbol{B},\hat{\boldsymbol{e}}(\boldsymbol{B}),\boldsymbol{w}(\boldsymbol{B}),\boldsymbol{M}(\boldsymbol{B}))$ parametrically dependent on the magnetization and renormalized by the electron-deformation interactions. Additional terms, depending on the external magnetic field and the temperature, change the response of rare earth ions on the field $\boldsymbol{B}$.

Table 2. Crystal field parameters $B_p^{\ k}$ (cm^{-1}) for the R^{3+} ions in $LiRF_4$ (R=Ho, Dy, Tb) crystals.

$B_p^{\ k}$	$LiTbF_4$ This work	$LiTbF_4$ [8]	$LiDyF_4$ [10]	$LiHoF_4$ [10]
$B_2^{\ 0}$	200	200	170	219.7
$B_4^{\ 0}$	-100.5	-100	-85	-87.3
$B_6^{\ 0}$	-2	-3.6	-4.2	-3.55
$B_4^{\ 4}$	-694	-1103	-721	-710
$B_4^{\ -4}$	-829	0	-661	-612
$B_6^{\ 4}$	-435	-529	-390	-387
$B_6^{\ -4}$	-283	0	-248	-253.7

Calculations are essentially simplified when making use of symmetry properties of a system. We worked with linear combinations of the deformation tensor $e(A_g^1)=e_{zz}$, $e(A_g^2)=(e_{xx}+e_{yy})/2$, $e(B_g^1)=e_{xx}-e_{yy}$, $e(B_g^2)=e_{xy}$, $e_1(E_g)=e_{xz}$, $e_2(E_g)=e_{yz}$) and the sublattice displacements corresponding to irreducible representations $\Gamma=A_g, B_g, E_g$ of the lattice factor group C_{4h}. In particular, the magnetic field $\boldsymbol{B}$ directed along the crystal symmetry *c*-axis brings about only totally symmetric A_g deformations, but the field in the *ab*-plane induces A_g and rhombic B_g deformations. The corresponding internal A_g and B_g deformations are described by three and five independent linear combinations of the sublattice displacements, respectively. We can write the electron-deformation interaction in the basis of symmetrical strains as follows

$$H_{ed}=\sum_{\Gamma\lambda}[\sum_{k}V_k(\Gamma^\lambda)e_k(\Gamma^\lambda)+\sum_{p}V_p^{"}(\Gamma^\lambda)\Delta w_p(\Gamma^\lambda)], \tag{7}$$

where $e_k(\Gamma^\lambda)$ and $\Delta w_p(\Gamma^\lambda)$ are independent variables. In case of coupling with A_g and B_g strains, the electronic operators equal

$$V(A_g^\lambda) = a^0_{\lambda,2}O^0_2 + a^0_{\lambda,4}O^0_4 + a^4_{\lambda,4}O^4_4 + a^{-4}_{\lambda,4}O^{-4}_4 + a^0_{\lambda,6}O^0_6 + a^4_{\lambda,6}O^4_6 + a^{-4}_{\lambda,6}O^{-4}_6, \quad (8)$$

$$V(B_g^\lambda) = b^2_{\lambda,2}O^2_2 + b^{-2}_{\lambda,2}O^{-2}_2 + b^2_{\lambda,4}O^2_4 + b^{-2}_{\lambda,2}O^{-2}_4 + b^2_{\lambda,6}O^2_6 + b^{-2}_{\lambda,6}O^{-2}_6 + b^6_{\lambda,6}O^6_6 + b^{-6}_{\lambda,6}O^{-6}_6. \quad (9)$$

The coupling constants $a^p_{\lambda,k}$ and $b^p_{\lambda,k}$ determined from piezospectroscopic measurements of the rare earth doped $LiYF_4$ crystals are given in table 1. We used in calculations the compliance constants of $LiYF_4$: $S(A_g11) = 7.78\cdot10^{-12}$, $S(A_g12) = -2.33\cdot10^{-12}$, $S(A_g22) = 3.36\cdot10^{-12}$, $S(B_g11) = 37.1\cdot10^{-12}$, $S(B_g12) = 8.0\cdot10^{-12}$, $S(B_g22) = 14.4\cdot10^{-12}$ (in units of m^3/J) [18], components of tensors $\hat{\boldsymbol{a}}$ and $\hat{\boldsymbol{b}}$ were calculated using parameters of a rigid ion model of the $LiYF_4$ lattice dynamics [19].

Components of the magnetic moment of a rare earth ion satisfy to self-consistent equations

$$m_\alpha = \sum_i \mu_B < i | L_\alpha + 2S_\alpha | i > e^{-E_i(\boldsymbol{M})/k_BT} (\sum_i e^{-E_i(\boldsymbol{M})/kT})^{-1}, \quad (10)$$

where $E_i(\boldsymbol{M})$ are the crystal energies (eigenvalues of the Hamiltonian H_{eff}), T – temperature, k_B is the Boltzman constant. To obtain crystal field energies and the magnetization $\boldsymbol{M} = n\boldsymbol{m}/v_0$, the following actions are performed: the matrix of the effective Hamiltonian with $\boldsymbol{M}$=0, $\hat{\boldsymbol{e}}$ =0, $\boldsymbol{\Delta w}$=0 is diagonalized, and the macro- ($\hat{\boldsymbol{e}}$ ($\boldsymbol{B}$)) and microdeformations ($\boldsymbol{\Delta w}(\boldsymbol{B})$), and components (10) of the magnetic moment are calculated. At the next step, the obtained values of $\boldsymbol{M}$, $\hat{\boldsymbol{e}}$, $\boldsymbol{\Delta w}$ are substituted into the Hamiltonian H_{eff}, and the procedure is repeated (up to seven times) to get a steady solution.

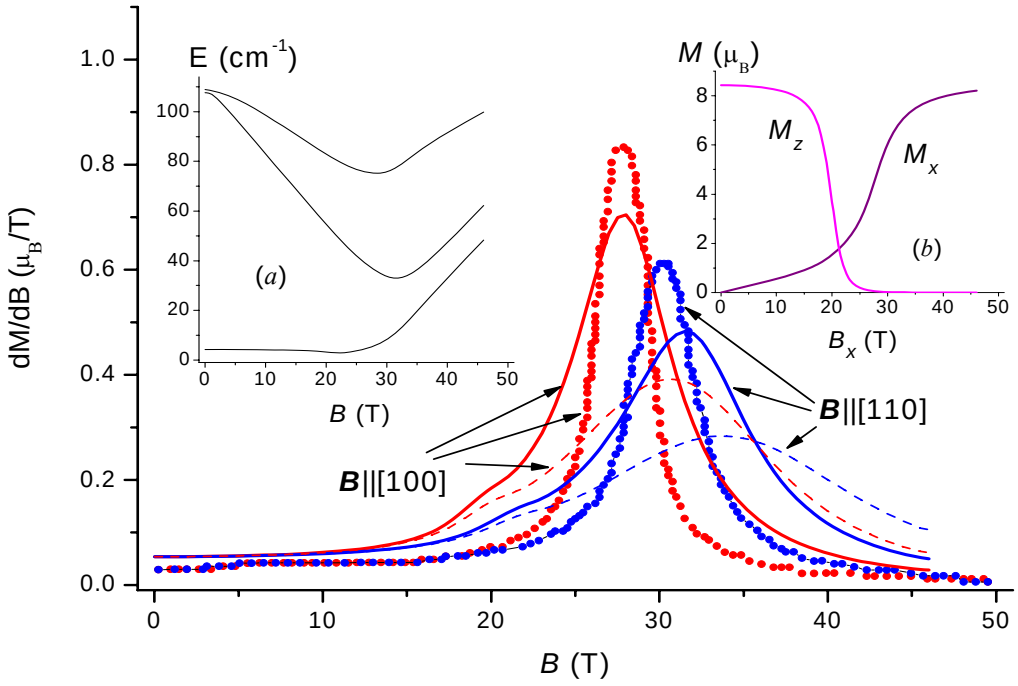

Figure 1. Differential magnetic susceptibilities of $LiTbF_4$ single crystals in magnetic fields $\boldsymbol{B}$||[100] and $\boldsymbol{B}$||[110] (in red and blue, respectively), T=1.4 K. Symbols – experimental data digitized from Ref. [12], solid and dashed curves represent the results of calculations carried out with or without taking into account the magnetoelastic interactions, respectively. Inset (a) – calculated energies of the three lower sublevels of the $^7F_6$ multiplet relative to the ground state vs. the magnetic field $\boldsymbol{B}$||[110]. Inset (b) – calculated magnetization components along (induced moment M_x) and normal (spontaneous moment M_z) to the external field $\boldsymbol{B}$||[100] vs. the field intensity.

Table 3. Energy levels (cm^{-1}) of the Tb^{3+} ion in $LiTbF_4$ and $LiYF_4$.

Multiplet, symmetry		Experimental energy levels		Calculated energies
		$LiTbF_4$ [6, 20]	$LiYF_4$:Tb [8,21]	
$^7F_6$	Γ_2	0	0	0
	Γ_2	1.0	0.9	0.97
	$\Gamma_{3,4}$	107	98	107
	Γ_1	124		114
	Γ_2	136		128
	$\Gamma_{3,4}$	166		169
	Γ_1	217		220
	Γ_1			344
	$\Gamma_{3,4}$			355
	Γ_2		360	363
$^7F_5$	Γ_2		2110	2120
	$\Gamma_{3,4}$			2133
	Γ_1			2169
	Γ_1			2174
	$\Gamma_{3,4}$		2196	2199
	Γ_1			2353
	$\Gamma_{3,4}$			2391
	Γ_2		2400	2401
$^7F_4$	Γ_1			3348
	$\Gamma_{3,4}$			3385
	Γ_2			3413
	Γ_2			3524
	Γ_1			3526
	$\Gamma_{3,4}$			3600
	Γ_1			3784
$^7F_3$	Γ_2	4333		4337
	$\Gamma_{3,4}$	4406		4406
	Γ_1	4473		4468
	$\Gamma_{3,4}$	4524		4509
	Γ_2	4532		4517
$^7F_2$	Γ_1	5035		5033
	Γ_2	5067		5071
	$\Gamma_{3,4}$	5285		5274
	Γ_2	5385		5366
$^7F_1$	Γ_1	5592		5592
	$\Gamma_{3,4}$	5690		5691
$^7F_0$	Γ_1	5917		5874
$^5D_4$	Γ_1	20561	20554	20567
	$\Gamma_{3,4}$	20571	20559	20559
	Γ_2			20569
	Γ_1	20580	20568	20590
	Γ_2			20626
	$\Gamma_{3,4}$	20641	20627	20640
	Γ_1	20654	20645	20661

Crystal field parameters (see table 2) were determined by fitting the calculated crystal field energies to the energy levels determined from the optical and EPR spectra [6, 20] of $LiTbF_4$. As it is seen in table 2, our parameters B_2^0, B_4^0, B_6^0, $[(B_4^4)^2+(B_4^{-4})^2]^{1/2}$=1081 cm^{-1} and $[(B_6^4)^2+(B_6^{-4})^2]^{1/2}$=519 cm^{-1} differ only slightly from corresponding parameters determined in [8] for the impurity Tb^{3+} ions in $LiYF_4$ (note that in [8] instead of the point S_4 symmetry, the D_{2d} symmetry was assumed). The B_2^0 parameter is fixed by the measured splitting of the $^7F_1$ multiplet. The calculated energies of sublevels of the $^7F_6$, $^7F_3$ and $^7F_2$ multiplets (see table 3) agree satisfactorily with the measured energies, however, large differences remain between the results of calculations and the experimental data for the $^5D_4$ multiplet. In particular, reversed positions of the two lower $^5D_4$ sublevels $\Gamma_{3,4}$ and Γ_1 are predicted by our set of parameters, as well as by all other published sets [6-9, 11].

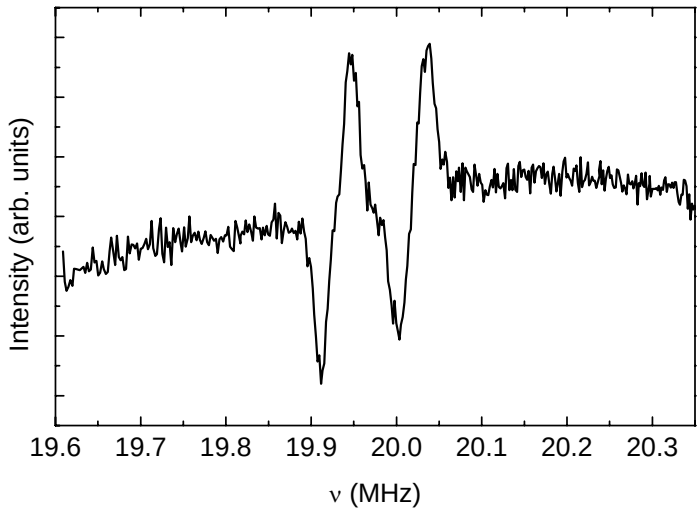

Figure 2. ^{19}F NMR spectrum of $LiTbF_4$ in the magnetic field B=0.5 T at room temperature ($\boldsymbol{B}\perp$c, φ=50^o).

To determine ratios of the parameters B_p^4 and B_p^{-4} (p=4 and 6), we analyzed presented in [12] dependences of the longitudinal magnetization in $LiTbF_4$ on the external pulsed magnetic fields applied to the oriented samples (rectangular rods with dimensions of 1.5×1.5×2.5 mm^3) in the *ab*-plane along the [100] and [110] directions (coinciding with the long edge of a rod) at the temperature 1.4 K. The magnetic field varied from zero up to 50 T during 20 μs, and we calculated the magnetization assuming, similarly to the authors of [12], the adiabatic process. Changes of the temperature ΔT of the magnetic subsystem induced by the increase of the field with steps $\Delta\boldsymbol{B}$ were calculated using the expression

$$\Delta T = -T\frac{<H_{eff}(\boldsymbol{B})\boldsymbol{m}>-<H_{eff}(\boldsymbol{B})><\boldsymbol{m}>}{<H_{eff}(\boldsymbol{B})^2>-<H_{eff}(\boldsymbol{B})>^2}\Delta\boldsymbol{B}\,. \qquad (11)$$

There are two terbium ions, Tb1 and Tb2, with coordinates $\boldsymbol{r}$(Tb1)=(0, 0, c/2), $\boldsymbol{r}$(Tb2)=(0, a/2, -c/4) in the unit cell. According to neutron scattering data [2] at 100 K, the lattice constants of $LiTbF_4$ equal a=0.5181, c=1.0873 nm. In the magnetically ordered state, the local field at the terbium ion Tbη (η=1, 2) is written as follows

$$B_{loc,\alpha}(Tb\eta) = B_\alpha + \sum_\beta[\sum_{\eta'=1,2} Q_{Tb\eta,Tb\eta'}(\alpha\beta) + 2\frac{4\pi}{3v}(\lambda - N_\alpha)\delta_{\alpha\beta}]m_\beta(Tb)\,. \qquad (12)$$

Here the demagnetizing factors of the rods are N_x=N_y=0.68 [22], N_z=0 (for the domains in the system with the dominant dipole-dipole interactions), the lattice sums $Q_{Tb\eta,Tb\eta}(xx) = Q_{Tb\eta,Tb\eta}(yy) = 1.18053$,

$Q_{Tb\eta,Tb\eta}(zz)=0.63894$, $Q_{Tb1,Tb2}(xx)=Q_{Tb1,Tb2}(yy)=0.41738$, $Q_{Tb1,Tb2}(zz)=2.16525$ (in units of $4\pi/3v$) have been computed by the Ewald method, the value of the isotropic exchange (antiferromagnetic) field constant λ=-0.316 have been determined previously in [11]. To account for the ordering of magnetic moments along the *c*-axis, a small initial external field of 0.01 T has been introduced. With the increasing magnetic field normal to the magnetic easy axis [001], the gap between the lower sublevel of the first excited Γ_{34} state and the ground quasi-doublet quickly diminishes (see Inset (*a*) in figure 1), and the peaks in the differential magnetic susceptibility are observed at the anticrossing point. As an example, evolutions of the spontaneous magnetic moment with the increasing transversal external field and of the induced moment along the field are shown in Inset (b) in figure 1.

As it is seen in figure 1, the differential susceptibilities computed with our set of the crystal field parameters match satisfactorily experimental data. However, the widths of the calculated peaks are much broader than the measured ones. It is evident that more elaborated study of the quantum phase transition in $LiTbF_4$ in the transversal magnetic fields beyond the mean field approximation is necessary. A comparison of the solid and dashed curves in figure 1 shows that magnetoelastic interactions contribute substantially into the magnetization if magnetic field is strong enough.

3. Experimental results and simulations of the NMR frequencies

The unit cell of $LiRF_4$ contains eight fluorine ions. Each of the two magnetically non-equivalent subsystems (labeled below by *s*=1, 2) of ^{19}F nuclei in the external magnetic field lying in the *ab*-plane involve four F^- sublattices with the following basis vectors $\boldsymbol{r}_k(s)$: $\boldsymbol{r}_1(1)$=(*ax, ay, cz*), $\boldsymbol{r}_2(1)$=(*-ax,- ay, cz*), $\boldsymbol{r}_3(1)$=(*ax, a*(*y*-0.5)*, c*(0.25-*z*)), $\boldsymbol{r}_4(1)$=(*-ax, -a*(*y*-0.5)*, c*(0.25-*z*)); $\boldsymbol{r}_1(2)$=(*-ay, ax,-cz*), $\boldsymbol{r}_2(2)$=(*ay, -ax,-cz*), $\boldsymbol{r}_3(2)$=(*-a*(*y*-0.5)*, ax, -c*(0.25-*z*)), $\boldsymbol{r}_4(2)$=(*a*(*y*-0.5)*, -ax, -c*(0.25-*z*)). At 295 K, the lattice structure constants of $LiTbF_4$ equal *a*=0.5192, *c*=1.0875 nm, *x*=0.2802, *y*=0.1619, *z*=0.0810 [2].

Single crystal of $LiTbF_4$ was grown using Bridgman-Stockbarger method. After axes definition by using X-ray diffractometer, it was shaped as a sphere to obtain the homogeneous demagnetizing field. The angular dependence of ^{19}F NMR spectrum was obtained by using homebuilt CW NMR spectrometer with a frequency sweep. The external magnetic field of 0.5 T was oriented in the basis plane of $LiTbF_4$. An example of the recorded spectrum is shown in figure 2 where two lines correspond to magnetically non-equivalent fluorine sites. The measured angular dependences of the resonance frequencies are represented in figure 3.

Table 4. Dipole lattice sums (in units of $4\pi/3v$)

$\alpha\beta$	*xx*	*xy*	*xz*	*yy*	*yz*	*zz*
$Q_{Tb1,F_1(1)}(\alpha\beta)$	0.1971	2.8226	-1.7445	3.8486	-2.3506	-1.0458
$Q_{Tb1,F_3(1)}(\alpha\beta)$	0.1925	-1.3327	-3.1669	-0.7825	2.4262	3.5900

According to expression (6), the local magnetic fields at the ^{19}F nuclei in $LiTbF_4$ in the paramagnetic phase equal (in the crystallographic frame)

$$B_x(F_k(s))=B_{loc,x}(ks)=B_x+[Q_{Tb1,F_k(s)}(xx)+Q_{Tb2,F_k(s)}(xx)+\varepsilon_{xx}(ks)-2\frac{4\pi}{3v}N]m_x+ [Q_{Tb1,F_k(s)}(xy)+Q_{Tb2,F_k(s)}(xy)+\varepsilon_{xy}(ks)]m_y, \quad (13)$$

$$B_y(F_k(s))=B_{loc,y}(ks)=B_y+[Q_{Tb1,F_k(s)}(xy)+Q_{Tb2,F_k(s)}(xy)+\varepsilon_{yx}(ks)]m_x+ [Q_{Tb1,F_k(s)}(yy)+Q_{Tb2,F_k(s)}(yy)+\varepsilon_{yy}(ks)-2\frac{4\pi}{3v}N]m_y. \quad (14)$$

The independent dipole lattice sums have been calculated by the Ewald method and are given in table 4. Components of tranferred hyperfine interaction tensors $\varepsilon_{\alpha\beta}(ks)$ have been considered as the fitting

parameters. Note that tensors $\varepsilon_{\alpha\beta}(ks)$ contain contributions due to the transferred hyperfine interactions between a ^{19}F nucleus and a couple of the nearest neighbor terbium ions, Tb1 and Tb2. The dipole sums and tensors $\hat{\varepsilon}(ks)$ satisfy the symmetry relations, in particular, $Q_{Tb1,F_1(2)}(xx) = Q_{Tb1,F_1(1)}(yy)$, $Q_{Tb1,F_1(2)}(yy) = Q_{Tb1,F_1(1)}(xx)$, $Q_{Tb1,F_1(2)}(xy) = -Q_{Tb1,F_1(1)}(xy)$, $\varepsilon_{xx}(12) = \varepsilon_{yy}(11)$, $\varepsilon_{yy}(12) = \varepsilon_{xx}(11)$, $\varepsilon_{xy}(12) = -\varepsilon_{xy}(11)$, $Q_{Tb2,F_1(1)}(\alpha\beta) = Q_{Tb1,F_3(1)}(\alpha\beta)$, $Q_{Tb2,F_3(1)}(\alpha\beta) = Q_{Tb1,F_1(1)}(\alpha\beta)$ for $\alpha, \beta = x, y$.

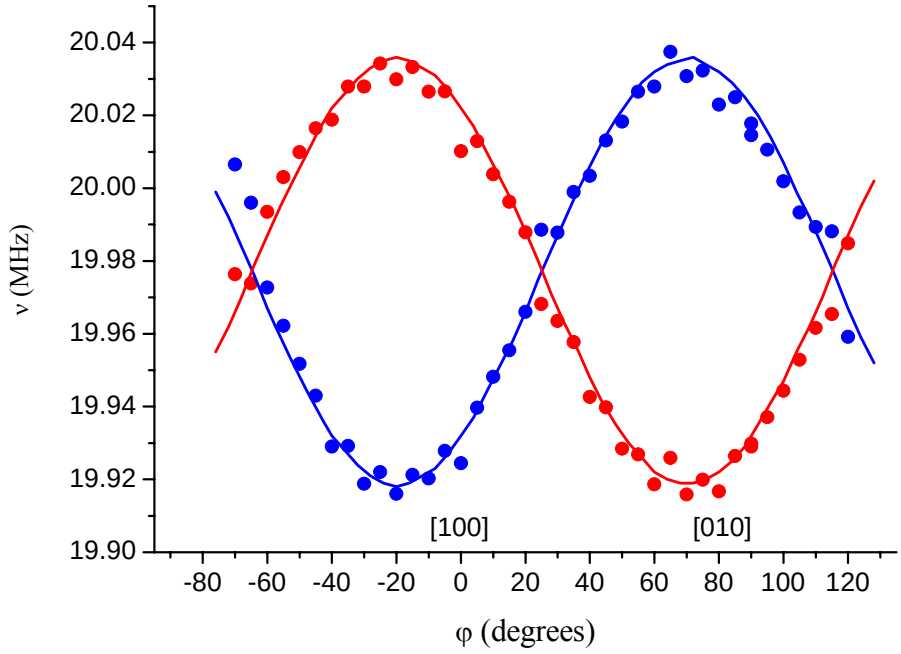

Figure 3. The angular dependence of ^{19}F NMR spectra in $LiTbF_4$ in the magnetic field of 0.5 T ($\boldsymbol{B}\perp$c), T=295 K. The circles are the experimental points, solid curves represent the results of calculations where the transferred hyperfine interaction parameters obtained in the present work have been used.

Three independent parameters, $\varepsilon_{xx}(11)$=-1.743, $\varepsilon_{xy}(11)$=-0.279 and $\varepsilon_{yy}(11)$=-1.481 (in units of $4\pi/3\nu$) were found from fitting the calculated resonance frequencies of ^{19}F nuclei $\nu(s) = \gamma_F[B_{loc,x}(1s)^2 + B_{loc,y}(1s)^2]^{1/2}$ (here $\gamma_F/2\pi$=40.07 MHz/T is the fluorine gyromagnetic ratio) to the results of measurements. The obtained hyperfine interaction constants are compared with the ones presented in [2] in table 5.

Table 5. Tranferred hyperfine interaction constants for $LiTbF_4$, g/cm^3 (M is the mass per formula unit).

	This work, accuracy ±1 g/cm^3	Ref. [2], accuracy ±3 g/cm^3
$M\varepsilon_{xx}(11)$	-22.38	-18.15
$M\varepsilon_{xy}(11)$	-4.35	0.11
$M\varepsilon_{yy}(11)$	-17.22	-19.49

4. Conclusion

In the present work corrected set of the crystal field parameters for the Tb^{3+} ions in $LiTbF_4$ have been obtained from the analysis of the literature data on the crystal field energies and the differential magnetic susceptibilities in high pulsed magnetic fields. We argue that magnetoelastic interactions contribute remarkably into formation of the magnetization in high magnetic fields. The obtained crystal field parameters correlate with the parameters determined earlier for isomorphic rare earth compounds.

Angular dependence of ^{19}F NMR spectra in the magnetic field perpendicular to the crystal *c*-axis has been measured and the corrected set of tranferred hyperfine interaction constants for $LiTbF_4$ has been determined. Diagonal components of the transferred hyperfine interaction tensor are similar to, but the nondiagonal component is much larger than corresponding parameters obtained earlier in [2]. The constants of the transferred hyperfine interaction and of the magnetic dipole-dipole interaction between the fluorine nuclei and the terbium ions in $LiTbF_4$ have comparable magnitudes (similar conclusions were obtained in the studies of superhyperfine structures of EPR spectra in dilute paramagnets $LiYF_4:Yb^{3+}$ [23], $LiYF_4:Nd^{3+}$ [24]), but different signs.

Acknowledgements

The authors are grateful to V. A. Shustov for the X-Ray orientation of the samples. This work was partially supported by the Ministry of Education and Science of the Russian Federation (project no. 13.G25.31.0025) and by the RFBR grant №09-02-00930.

References

[1] Aminov L K, Malkin B Z and Teplov M A 1996 *Handbook on the Physics and Chemistry of Rare Earths,* vol.22 (Amsterdam: North-Holland)
[2] Als-Nielsen J, Holmes L M, Larsen F K and Guggenheim H J 1975 *Phys. Rev*. B **12** 191
[3] Hansen P E and Nevald R 1977 *Phys. Rev*. B **16** 146
[4] Hansen P E, Johanson T and Nevald R 1975 *Phys. Rev.* B **12** 5315
[5] Nevald R and Hansen P E 1977 *Physica* B **86-88** 1443
[6] Christensen H P 1978 *Phys. Rev*. B **17** 4060
[7] Krotov V I, Malkin B Z and Mittelman A A 1982 *Physics of the Solid State* (St Petersburg) **24** 542
[8] Liu G K, Carnall W T, Jones R P, Cone R L and Huang J 1994 *J. Alloys Compounds* **207-208** 69
[9] Liu G K 2005 *Spectroscopic Properties of Rare Earths in Optical Materials* Eds Guokui Liu and Bernard Jacquier (Springer Series in Materials Science, vol. 83) pp 1-89
[10] Romanova I V, Abdulsabirov R Yu, Korableva S L, Malkin B Z, Mukhamedshin I R, Suzuki H and Tagirov M S 2006 *Magn. Resonance in Solids EJ* **8** 1
[11] Romanova I V, Malkin B Z, Mukhamedshin I R, Suzuki H and Tagirov M S 2002 *Physics of the Solid State* (St Petersburg) **44** 1475
[12] Kazei Z A, Snegirev V V, Abdulsabirov R Yu, Korableva S L, Broto J M and Rakoto H 2006 *Proceedings of 34 Conference on Low Temperature Physics*, part 1, p. 13
[13] Altshuler S A and Kozyrev B M 1972 *Electron paramagnetic resonance* (Moscow: Nauka)
[14] Abdulsabirov R Yu, Kazantsev A A, Korableva S L, Malkin B Z, Nikitin S I and Stolov A L 2006 *J. Lumin*. **117** 225
[15] Abdulsabirov R Yu, Kazantsev A A, Korableva S L, Malkin B Z, Nikitin S I, Stolov A L, Tagirov M S, Tayurskii D A and van Tol J 2002 *SPIE Proceedings* **4766** 59
[16] Aminov L K and Malkin B Z 2008 *Dynamics and kinetics of electronic and spin excitations in paramagnetic crystals (*Kazan: Kazan State University)
[17] Bertaina S, Barbara B, Giraud R, Malkin B Z, Vanuynin M V, Pominov A I, Stolov A L and Tkachuk A M 2006 *Phys. Rev.* B **74** 184421
[18] Blanchfield P and Saunders G A 1979 *J. Phys.* C **12** 4673

[19] Salaun S, Bulou A, Rousseau M, Hennion B and Gesland G Y 1997 *J. Phys.:Condens. Matter* **9** 6957
[20] Magarino J, Tuchendler J, Beauvillain P and Laursen I 1980 *Phys. Rev.* B **21** 18
[21] Liu G K, Huang J, Cone R L and Jacquier B 1988 *Phys. Rev.* B **38** 11061
[22] Sato M and Ishii Y 1989 *J. Appl. Phys.* **66** 983
[23] Aminov L K, Ershova A A, Zverev D G, Korableva S L, Kurkin I N and Malkin B Z 2008 *Appl. Magn. Res*. **33** 351
[24] Aminov L K, Ershova A A, Korableva S L, Kurkin I N, Malkin B Z and Rodionov A A 2011 *Physics of the Solid State* (St Petersburg) **53** 2129